

EFFECT OF DEPOSITION TEMPERATURE VARIATION ON THIN FILMS SYNTHESIS VIA AACVD

T. SHUJAH^{a*}, A. BUTT^a, M. IKRAM^b, S. SHABBIR^c, S. ALI^{a,b}

^a*Material and Nanoscience Research Lab. (MNRL), Department of Physics, Government College University, Lahore, 54000, Pakistan.*

^b*Solar Applications Research Lab, Department of Physics, Government College University, Lahore, 54000, Pakistan.*

^c*Fatima Jinnah Women University, Old Presidency, The Mall, Rawalpindi 46000, Pakistan.*

In this study, ZnO-SnO₂ composite thin films were deposited onto glass substrate via aerosol assisted chemical vapor deposition (AACVD) technique at various deposition temperatures. Effect of deposition temperature on structural, morphological, compositional and optical properties of thin film were studied by using X-ray diffraction (XRD), Scanning electron microscopy (SEM), Rutherford backscattering spectroscopy (RBS) and UV-Vis Diffuse Reflectance Spectroscopy (DRS). Results showed the successful deposition of Zn₂SnO₄ at 450°C. At 350°C, only ZnO was deposited while SnO₂ was observed along with Zn₂SnO₄ at the deposition temperature of 400°C. The synthesis technique, for its simplicity and low cost, is not only industrially attractive technique but also represents a more environmentally sustainable way for the production of nano devices with controlled stoichiometry.

Received June 8, 2016; Accepted August 17, 2016)

Keywords: AACVD, Thin Film, Nanostructures, Deposition temperature, Zn₂SnO₄

1. Introduction

Several techniques for the synthesis of 1-D metal oxide nanostructures have been developed. These techniques can basically be divided into two categories: vapor-phase synthesis and solution-phase synthesis [1]. Vapor phase methods include chemical vapor deposition (CVD), metal organic CVD [2, 3], thermal evaporation [4], and catalyst assisted laser ablation [5]. All these methods are performed at high temperature and control very well the diameter, composition, and morphology of the 1-D metal oxide nanostructures. Solution phase methods require only ambient temperature and reduce the fabrication complexity and cost.

This paper focuses on the growth of metal oxide nanostructures via aerosol assisted chemical vapor deposition (AA-CVD). The application of a chemical method in which the NPs are synthesized in a single step is potentially advantageous. Synthesizing NPs in the gas phase have many advantages over liquid phase synthesis including greater purity and continuous mode of operation but also involves a number of challenges, including the controlled and homogeneous deposition of nanoparticles onto surfaces and the chemical modification of individual nanoparticles [6]. The use of aerosols for NPs synthesis is well known. By adjusting the process parameters, we can easily control the particle size, crystallinity, chemical homogeneity and stoichiometry. Together in a single AACVD process, these two techniques could overcome the challenges associated with gas phase NP synthesis [7].

Zinc oxide (ZnO) and Tin dioxide (SnO₂) are n-type semiconductors with wide band gap of 3.5 eV and 3.3 eV respectively. Both oxides have outstanding optical, electrical and mechanical properties. Because of their high optical transparency in the visible region, good electrical

*Corresponding author: tahira_gcu@hotmail.com

conductivity and high infrared reflectivity, ZnO and SnO₂ are the most attractive materials for gas sensor applications, as a catalyst and as transparent conductive oxides for solar cell applications.

The aim of this work was to investigate the use of aerosol assisted chemical vapor deposition (AACVD) technique to synthesize SnO₂-ZnO composite nano thin films onto glass substrate. In particular to see how deposition temperature variation affects thin film growth and preferred orientation.

2. Principles and characteristics of AA-CVD

AA-CVD is a variant of traditional CVD. The process is based on the atomization of a liquid precursor solution, kept in a glass flask, into aerosol droplets. These droplets are transported to the heated reaction zone by a flow of carrier gas. In the reaction zone, the solvent undergoes rapid evaporation and/or decomposition, forming the precursor vapors. These precursor vapors react and decompose to form the desired product on top of the heated substrate. Two kinds of chemical reactions (heterogeneous/homogeneous) can occur in the reaction chamber. In first case vaporized precursor decomposes in the gas phase leading to the formation of intermediate species which then adsorb to the surface. Further decomposition and heterogeneous reaction results in the formation of thin film of desired material. While at higher temperature, earlier decomposition of the precursor vapor occur leading to homogeneous nucleation of particle which results in the deposition of porous film on the substrate surface. The exhaust is vented from the reactor through an extraction system [8,9]. Figure 1 show the reaction process involved in AACVD reaction.

The main criteria for the selection of the solvent are high solubility of the precursor, low vapor pressure and low viscosity. Precursor can be atomized using different types of aerosol generators such as pneumatic aerosol jet, electrostatic atomization and ultrasonic aerosol generation. Ultrasonic generation is the option adopted in our work. Nitrogen and argon are the most commonly used inert carrier gases. Compressed air is used for the deposition of oxide products, while reactive gases such as H₂ may also be used with other primary carrier gases to help the CVD reaction [10].

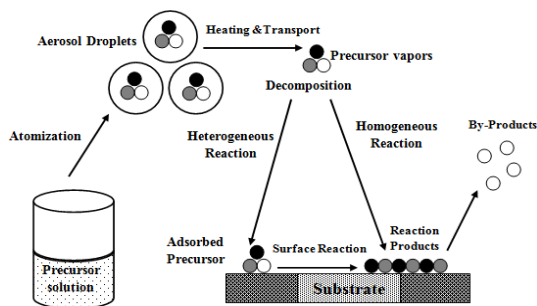


Fig. 1: Schematic illustration of the process involved in AACVD

The most significant features of AACVD making it a promising technique are:

- AACVD uses single source precursors which enables efficient molecular mixing of chemical precursors and allows synthesis of multi component material with controlled stoichiometry. Due to lesser diffusion distance between reactants and intermediates, films are rapidly deposited at relatively low temperature.
- It lowers the cost of deposition by using simple vapor precursor generation and delivery method, as compared to conventional method which uses a vaporizer/bubbler.
- AACVD can be performed in an open atmosphere, without using any sophisticated reactor or vacuum system e.g. for deposition of oxide and relatively less oxygen sensitive non-oxide materials, which also makes it a low cost process as compared to conventional method [11].

3. Experimental details

3.1 Growth of thin films

The synthesis of ZnO-SnO₂ composite nano thin films involved preparation of single precursor solution of zinc acetate Zn(CH₃COOH)₂·2H₂O and tin chloride SnCl₄·5H₂O in methanol solvent. Precursor solution was prepared by dissolving 0.1 moles of each zinc acetate and tin chloride in 15 ml of methanol (Sigma-Aldrich, ≥99.6%). Glass slides (10 mm×10 mm×1 mm) were used as substrates and cleaned with ethanol and then with acetone, dried in air and then placed inside the reactor at various deposition temperatures (350°C, 400°C and 450°C) to investigate the effect of variation in deposition temperature on the growth of nanostructures.

An ultrasonic humidifier was used to generate an aerosol from the precursor solutions, kept in a glass flask, which was transported to the heated substrate by a flow of carrier gas (compressed air). The flow was set to 200 cm³·min⁻¹. The exhaust from the reactor was vented directly into the extraction system of a fume cupboard. The deposition time was between 40 and 50 min, until all the precursor had passed through the reactor. Figure 2 shows the schematic diagram of experimental setup.

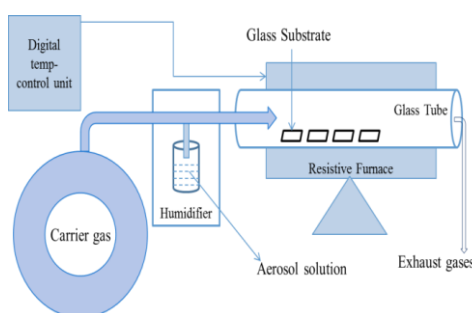


Fig. 2: Schematic drawing of the experimental setup

Three samples, S1, S2 and S3 were prepared according to the parameters described in Table 1.

Table 1: Synthesis parameter for the deposition of thin films via AACVD

Sample code	Molar concentrations of precursors Zn(CH ₃ COOH) ₂ ·2H ₂ O + SnCl ₄ ·5H ₂ O	Solvent (ml)	Gas Flow (cm ³ /min)	Deposition Temperature (°C)
S-1-1	0.1 M + 0.1 M	15	Compressed air 200	350
S-1-2	≐	≐	≐	400
S-1-3	≐	≐	≐	450

3.2 Material Characterization

The structural and phase analysis of film was performed using X-ray Diffraction (XRD) Bruker AXS D8-DISCOVER with CuK α radiation operated at 40 kV and 40 mA. Field Emission Scanning Electron Microscopy (FESEM) analysis was carried out on a Field Emission JEOL 6301F instrument using accelerating voltages of 5 kV for film morphology. Rutherford backscattering (RBS) was performed to investigate elemental analysis. Incident particles were He⁺⁺ ions accelerated by 5 MV pelletron tandem accelerators to energy of 2.084 MeV. Incident angle and backscattering angle were maintained at 0° and 170° respectively with detector resolution (20 keV). Optical properties were investigated using Perkinelmer Lambda 950 UV/Vis/NIR Spectrometer.

4. Results and Discussion

Figure 3 shows XRD pattern of thin films prepared by AACVD. Results for S-1-1 revealed the presence of diffraction peaks at 31.7 , 34.4 , 47.5 and 56.6° 2θ , which correspond to (100), (002), (102) and (110) planes in the hexagonal structure (ICDD card # 01-074-0534) of ZnO, with P63mc space group, $a=b=3.2499\text{\AA}$ and $c=5.2066\text{\AA}$, while $\beta=90^\circ$. Crystallite size calculated with scherrer formula is 80.5 nm .

XRD pattern of as-prepared thin film S-1-3, using AACVD, confirms growth of Zn_2SnO_4 with no impurity observed. As shown in the figure, all obtained diffraction peaks in the XRD pattern can be indexed to the cubic phase of Zn_2SnO_4 (ICDD card no. 00-024-1470), with space group Fd-3m, $a = b = c = 8.6574\text{\AA}$ while $\beta=90^\circ$. Crystallite size was calculated as 112 nm .

XRD pattern of S-1-2 revealed that along with Zn_2SnO_4 , peaks of SnO_2 corresponding to the tetragonal of ICDD card no. 01-077-0449) with space group P42/mnm, were also observed at 26.5 and $51.7^\circ 2\theta$. Crystallite size as calculated with scherrer formula is 156 nm .

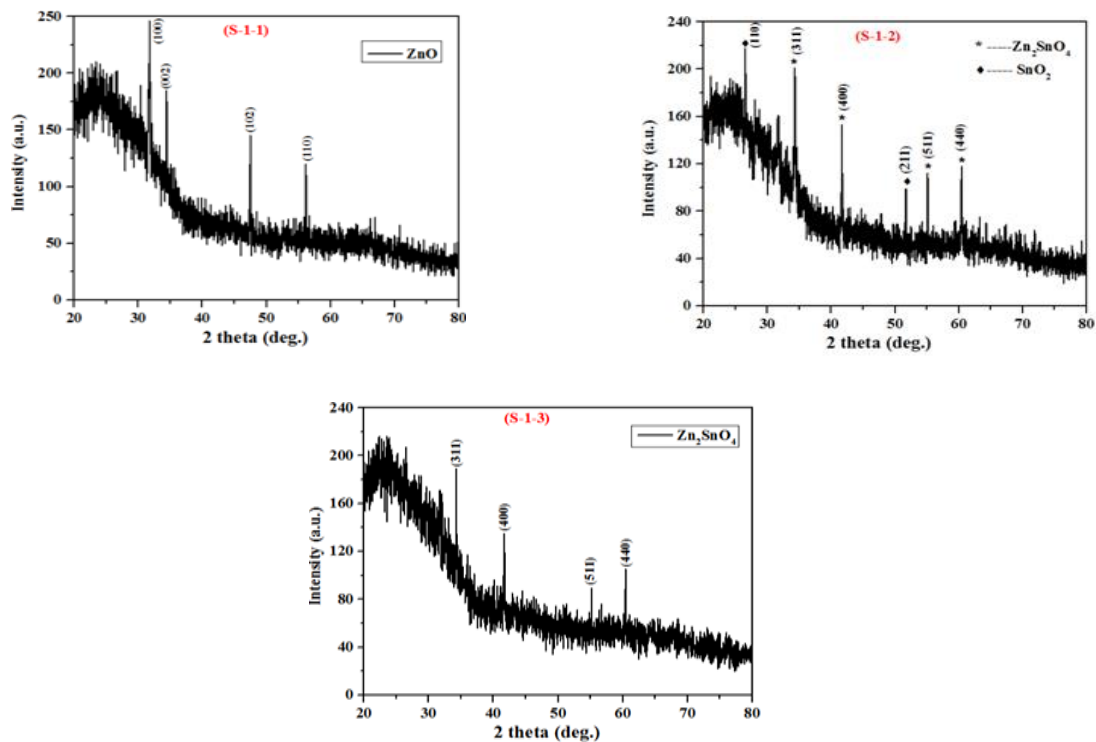


Fig. 3: XRD pattern of deposited thin films.

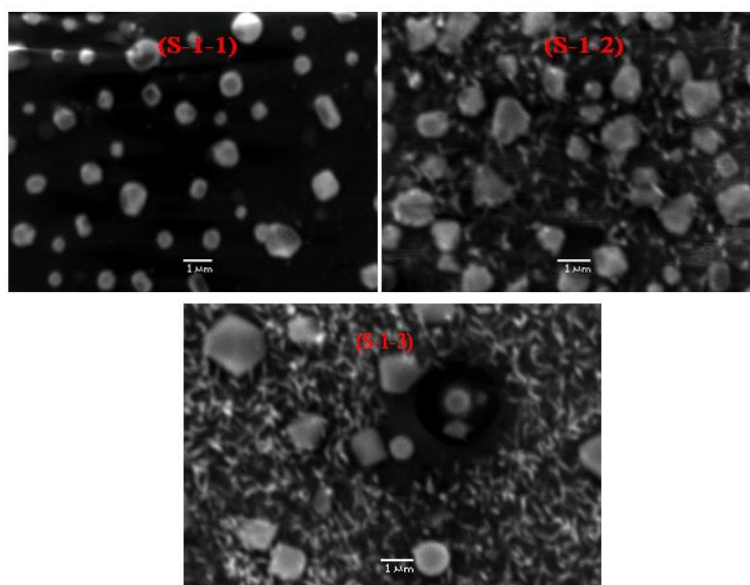


Fig. 4: SEM micrographs of grown thin films

The shape and morphology of the deposited films were determined at various magnifications as shown in Figure 4. The surface consisted mainly of spherical nanoparticles with a typical size of 100–600 nm. The SEM micrographs of grown films of zinc-tin oxide composite show fine granular deposition of metal oxide, covering the entire glass substrate, with some agglomeration of finer particulates to form bigger clusters depending upon deposition temperature. At lower temperature (350°C), discontinuous and low density films were obtained however these finely deposited particles provided nucleation zones for random multidirectional filamentous growth at 400°C. The high distribution of nucleation sites can encourage the formation of aligned structures and their lateral coalescence to form smooth continuous thin films [12]. Higher synthesis temperatures gave more defined films. At 450°C the filamentous growth became complex and a finely knit intricate film structure has led to the formation of dense porous microstructures with high spatial film density. Temperature is governing the morphological orientation of deposited precursors. At low temperature, decomposed aerosol precursors have covered substrate discontinuously in the form of particle. Increase in deposition temperature has encouraged particles growth in thread/filament shape giving highly continuous and porous thin films.

Figure 5 depicts the depth profile studies of deposited thin films using Rutherford back scattering analysis. The ‘Zn’ and ‘Sn’ are simulated at the channel energies corresponding to 1.6 and 1.8 MeV respectively. The analysis was carried out to get the percentage elemental composition of thin film as shown in Table 2. At 350 °C deposition temperature, only zinc and oxygen were observed to be deposited with film thickness of 150–200 nm. Film composition varied significantly with a change in deposition temperature. Film thickness was preserved at 400 °C with substantial amount of tin deposited along with zinc and oxygen. Further increase in deposition temperature had increased film thickness to ~300 nm but declined the deposited Zn concentration in thin film; however Sn concentration was augmented to 6.48%. The decline in Zn concentration at 450 °C can be attributed to the heterogeneous chemical reactions taking place inside reaction chamber, since chemical species present inside composite behave differently at different deposition temperature, some are lost at high temperature and others may coalesce to form complex film structure [13].

If RBS results are coupled with SEM and XRD results it can be implied that the particles deposited at 350 °C deposition temperature had only Zn and O as constituting elements for thin film, which means that ZnO is deposited at 350 °C and Small filamentous protrusions observed in SEM micrographs at 400°C are composed of SnO₂. Hence, it can be inferred that for the deposition

Zn₂SnO₄ composite by AACVD method minimum deposition temperature is 400 °C because below this temperature one of the component i.e. Sn will not deposit.

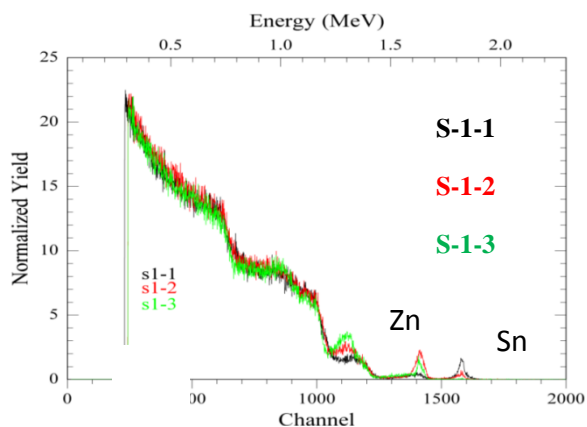


Fig. 5: RBS pattern of of thin films deposited at 350 °C, 400 °C and 450°C respectively

Table 2: Film thickness and percentage weight composition of thin films

Sample Code	Film Thickness (nm)	Zn (wt %)	Sn (wt %)	O (wt %)
S-1-1	150-200 nm	22.5 %	0.0 %	77.5%
S-1-2	150-200 nm	33.62 %	3.17 %	63.21 %
S-1-3	~ 300 nm	7.19 %	6.48 %	86.33 %

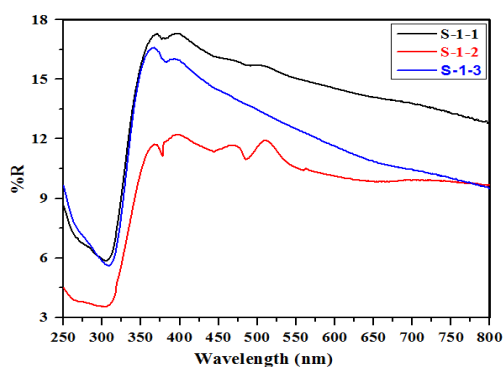


Fig. 6: Reflectance spectrum of as-deposited thin films.

Optical investigations were carried out using UV-Vis Diffuse Reflectance Spectroscopy (DRS). Figure shows reflectance of as-grown thin films as the function of wavelength. In sample S-1-1, a considerable reduction in reflectance starts at about 371 nm. Films deposited at 400°C and 450°C showed almost similar trend with a slightly shift of peaks towards lower wavelength: 366 nm and 364 nm for S-1-2 and S-1-3 respectively as shown in Figure 6. This shift may be attributed to the structural modification [14] as observed in SEM analysis.

For band gap measurements, DR spectra of the samples after Kubelka-Munk treatment is shown in the figure 7.

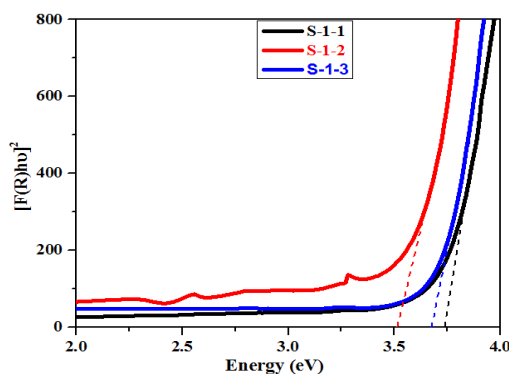


Fig. 7: Transformed kubelka- munk spectra of grown thin films

The optical absorption coefficient (α) is calculated using reflectance data according to the Kubelka-Munk equation,

$$F(R) = \alpha = (1-R)^2/2R,$$

Where

R= percentage of reflected light.

The incident photon energy ($h\nu$) and the optical band gap energy (E_g) are related to the transformed Kubelka- Munk function,

$$[F(R)h\nu]^n = A(h\nu - E_g),$$

Where

E_g =band gap energy,

A is the constant depending on transition probability and n is the power index that is related to the optical absorption process. Theoretically n equals to 1/2 or 2 for an indirect or a direct allowed transition, respectively [15].

Bandgap of the S-1-1, S-1-2 and S-1-3 are determined to be 3.74eV, 3.51eV, and 3.68eV respectively, based on the direct transitions, show slight deviation from the reported values for the bandgaps of ZnO and SnO₂. This can be justified by the fact that bandgap strongly depends upon the film thickness and grain size. So, we can slightly vary the band gap value by varying film thickness. In case of AACVD film thickness can be easily changed by varying different parameters involved in synthesis process [16].

Band gap decreased with the increase in deposition temperature from 350°C to 400°C, this may be justified by the fact that bandgap decrease with the increase in crystallite size, which is in agreement with XRD results. Increase in crystallite size may be attributed to the agglomeration of smaller particle resulting in the formation of larger grains with better crystallinity [17]. On further increase in deposition temperature to 450°C (S-1-3), band gap was dropped to lower value. This is probably because of presence of single phase of Zn₂SnO₄ in S-1-3 as compared to S-1-2 which possesses a combination of Zn₂SnO₄ and SnO₂.

5. Conclusion

ZnO-SnO₂ composite thin films were grown onto glass substrate at various deposition temperatures (350°C, 400°C and 450°C) via AACVD technique to investigate the effect of deposition temperature on film growth. As-deposited thin films were characterized for their structural, morphological, elemental and optical analysis using XRD, SEM, RBS, and DRS techniques. Results predicted the change in deposition temperature is governing phenomena for physical features of deposited thin film. Moreover, deposition temperature is a major factor in

growth rate control. Surface density of grown nanostructures and film thickness can be easily varied by altering deposition temperature in AACVD.

Overall AACVD allows a simplification in the synthesis of nanostructures while maintaining excellent control over their structural, morphological as well as optical properties of thin films.

Acknowledgements

The author would like to acknowledge Dr. Tajammul Hussain(late), at National Centre for Physics Islamabad (NCP),for guidance and support in this research.

References

- [1] M. M. Arafat, B.Dinan, S. A. Akbar, A. S. M. A. Haseeb,Sensors **12**, 7207 (2012).
- [2] C. Pflitsch, A. Muhsin, U. Bergmann, B. Atakan, Surface and Coatings Technology **201**, 73 (2006).
- [3] E. K. Nyutu, M. A. Kmetz, S. L. Suib,Surface and Coatings Technology **200**, 3980 (2006).
- [3] Z. R. Dai, Z. W. Pan, Z. L. Wang, Advanced Functional Materials **13**, 9 (2003).
- [4] Z. Liu, D. Zhang, S. Han, C. Li, T. Tang, W. Jin, C. Zhou,Advanced Materials **15**, 1754 (2003).
- [5] G. F. Fine, L. M. Cavanagh, A. Afonja R.Binions,Sensors **10**, 5469 (2010).
- [6] F. E. Annanouch, S.Vallejos, T.Stoycheva, C. Blackman, E. Llobet,Thin Solid Films **548**, 703 (2013).
- [7] P. Marchand, I. A. Hassan, I. P. Parkin, C. J. Carmalt,Dalton Transactions **42**, 9406 (2013).
- [8] X. Hou, K. L. Choy, Processing and Applications of Aerosol-Assisted Chemical Vapor Deposition. Chemical vapor deposition **12**, 583 (2006).
- [9] R. Binions, C. J. Carmalt, I. P.Parkin,Measurement Science and Technology **18**, 190 (2006).
- [10] K. L. Choy,Progress in materials science **48**, 57 (2003).
- [11] G. Shaw, I. P.Parkin, K.F. Pratt, D. E. Williams,Journal of Materials Chemistry **15**, 149(2005).
- [12] S. Vallejos, P.Umek, C. Blackman, Journal of nanoscience and nanotechnology **11**, 8214 (2011).
- [13] M. Soosen Samuel, L. Bose, L, K.C. George,Academic Review 1, 57(2009).
- [14] A. E. Morales, E. S. Mora, U.Pal,Revista Mexicana de Fisica S **53**, 18 (2007).
- [15] S. J. Moniz, R. Quesada-Cabrera, C. S. Blackman, J. Tang, P. Southern, P. M. Weaver, C. J. Carmalt,Journal of Materials Chemistry A **2**, 2922 (2014).
- [16] N. Ali, S.T.Hussain, Y. Khan, N. Ahmad, M. A.Iqbal, M. A, S. M. Abbas,Materials Letters, **100**, 148 (2013).